Chemistry Africa (2018) 1:17–28
https://doi.org/10.1007/s42250-018-0002-z

ORIGINAL ARTICLE

Synthesis and Characterization of Tetranuclear Metal Complexes with an Octadentate Azodye Ligand

Ashish Kumar Sarangi[1] · Bipin Bihari Mahapatra[2] · Sisir Kumar Sethy[2]

Received: 7 March 2018 / Accepted: 4 May 2018 / Published online: 23 May 2018

Abstract
An octadentate azodye ligand containing phenolic/ketonic oxygen and azo nitrogen donor atoms when complexed with divalent metal ions forms tetranuclear complexes of composition $[M_4LCl_4(H_2O)_{12}]$ and $[M'_4LCl_4(H_2O)_4]$ where, M = Co^{II},Cu^{II}, Ni^{II}, Mn^{II} and M′ = Zn ^{II,}, Cd^{II} and LH_4 = 4,4′-bis(2,4′-dihydroxy-5′-acylphenylazo)diphenylsulphone (BDHAPADPS). The metal complexes were characterised by analytical, magnetic moment, conductance, I.R., electronic spectra, thermal, ESI–MS, ESR, XRD, SEM and EDX. DFT calculations of the ligand and metal complexes have been made by GAUSSIAN 03 rev. A.01 programme package. The antibacterial study of the ligand and the complexes has been made using Gram positive and Gram negative bacteria.

Keywords Polydentate azodye ligand · SEM study · DFT calculations

1 Introduction

Azodyes are synthesized by coupling reaction of aromatic primary amines with aromatic hydroxyl compounds. Due to the presence of active azo (–N=N–) group they show a wide range of applications in various fields. 4,4′-diaminodiphenyl sulfone is an antibiotic used for the treatment of Leprosy [1]. It is also used for the treatment and prevention of pneumocystis pneumonia and toxoplasmosis and for the treatment of various types of skin diseases as acne, dermatitis herpetiformis [2]. Azodye have enormous applications in medical science as a potent antibacterial, antitumor and anti-inflammatory drugs and the pharmacological activity of these compounds is enhanced on complexation with various metal ions. We have reported a number of azodye ligands contaning nitrogen, oxygen and sulfur donor atoms and their mono, bi, tri, tetra, penta, hexa and octameric metal complexes [3–6]. In the present investigation, we describe here the preparation of one octadentate azodye ligand (Fig. 1) and its six tetrameric Co(II), Ni(II), Cu(II), Mn(II), Zn(II) and Cd(II) complexes.

✉ Ashish Kumar Sarangi
ashishsbp_2008@yahoo.com

Bipin Bihari Mahapatra
mahapatra.bipin@yahoo.com

[1] Department of Chemistry, Government College of Engineering Keonjhar, Keonjhar, Odisha 758002, India

[2] P.G. Department of Chemistry, G.M. University, Sambalpur, Odisha, India

2 Experimental

2.1 Materials

The metal chlorides used in this work are of SRL grade and 4,4′-diaminodiphenyl sulfone and 2,4-dihydroxyacetophenone are from Sigma Aldrich.

2.2 Synthesis of the Ligand

4,4′-Diaminodiphenyl sulfone (0.01 mol, 0.8 g.) was treated with a mixture of $NaNO_2$ and HCl. The resulting solution was added to an alkaline solution of 2,4-dihydroxyacetophenone (0.02 mol, 1.0 g.) at 0–5 °C, when the azodye 4,4′-bis(2,4′-dihydroxy-5′-acylphenylazo)diphenylsulphone (BDHAPADPS) was formed. $LH_4 = C_{28}H_{22}N_4SO_8$ (574.54), m.p. > 250 °C. Anal. Calc. (%) C, 58.5; H, 3.86; N, 9.7; S, 5.5; Found (%) C, 58.2; H, 3.5; N, 9.4; S, 5.4, IR (KBr pellet cm^{-1}): 1475 ν (C–O); 1607 ν (N=N); 1631 ν (C=O). $^{13}C\{^1H\}$ NMR δ: 26.0 (C-1), 103.0, 108.0, 115.0, 129.0, 130.0, 133.0 (Ar–C), 163.0 (C-4), 166.0 (C-6), 203.0 (C-2).

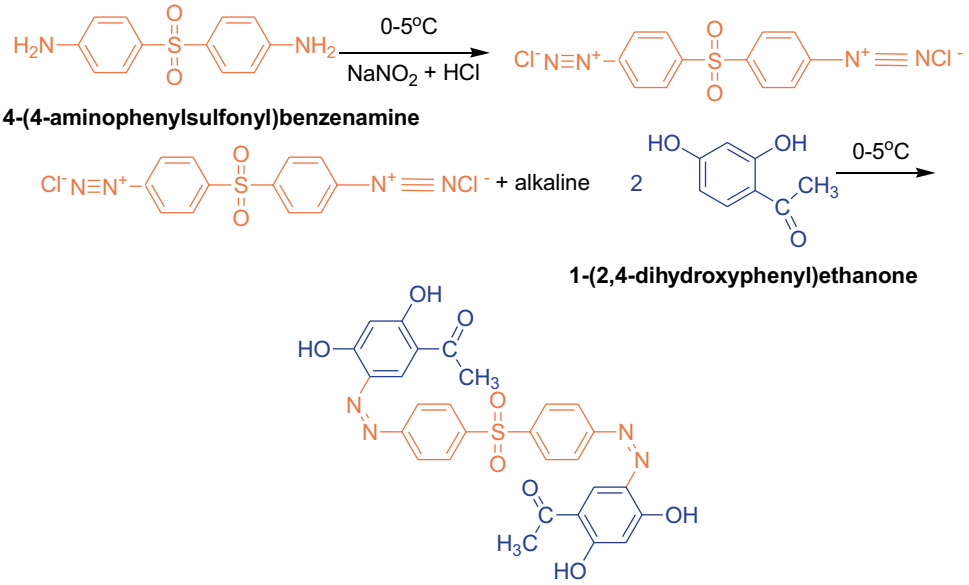

2.3 Synthesis of the Metal Complexes

An ethanolic solution of metal chloride was mixed with a solution of the ligand in ethanol in 4:1 ratio. The resulting solution is heated in a heating mantal to 50–60 °C for about 1 h and the pH is raised to ~ 7 by adding conc. NH_4OH drop by drop with stirring. Where upon metal complexes were precipitate out which were filtered out, washed with ethanol followed by ether and dried in vacuum.

$[Co_4(BDHAPADPS)Cl_4(H_2O)_{12}]$ (Dark brown) $C_{28}H_{42}Cl_4Co_4N_4O_{20}S$ (1163.7), m.p. > 250 °C, Anal Calc. (%) C, 28.8; H, 3.6; N, 4.8; S, 2.7; Cl, 12.2; Co, 20.2; Found (%) C, 28.5; H, 3.4; N, 4.6; S, 2.5; Cl, 12.0; Co, 19.8, IR (KBr pellet cm^{-1}): 1435 *ν* (C–O); 1499 *ν* (N=N); 1593 *ν* (C=O); 577 *ν* (M–O); 492 *ν* (M–N).

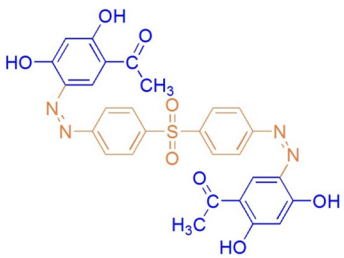

4,4/-bis(2,4/-dihydroxy-5/-acylphenylazo)diphenylsulphone

Fig. 1 A novel octadentate oxygen–nitrogen donor azodye ligand was made in this study

$[Ni_4(BDHAPADPS)Cl_4(H_2O)_{12}]$ (Light green) $C_{28}H_{42}Cl_4Ni_4N_4O_{20}S$ (1162.7), m.p. > 250 °C, Anal Calc. (%) C, 28.8; H, 3.6; N, 4.8; S, 2.7; Cl, 12.2; Ni, 20.1; Found (%) C, 28.5; H, 3.4; N, 4.5 S, 2.6; Cl, 12.0; Ni, 19.8, IR (KBr pellet cm^{-1}): 1434 *ν* (C–O); 1497 *ν* (N=N); 1590 *ν* (C=O); 575 *ν* (M–O); 490 *ν* (M–N).

$[Cu_2(BDHAPADPS)Cl_4(H_2O)_{12}]$ (Green) $C_{28}H_{42}Cl_4Cu_4N_4O_{20}S$ (1182.6), m.p. > 250 °C, Anal Calc. (%) C, 28.4; H, 3.5; N, 4.7; S, 2.7; Cl, 11.9; Cu, 21.4; Found (%) C, 28.2; H, 3.2; N, 4.5; S, 2.4; Cl, 11.7; Cu, 21.2, IR (KBr pellet cm^{-1}): 1436 *ν* (C–O); 1500 *ν* (N=N); 1589 *ν* (C=O); 575 *ν* (M–O); 488 *ν* (M–N).

$[Mn_4(BDHAPADPS)Cl_4(H_2O)_{12}]$ (Purple) $C_{28}H_{42}Cl_4Mn_4N_4O_{20}S$ (1148.2), m.p. > 250 °C, Anal Calc. (%) C, 29.2; H, 3.6; N, 4.8; S, 2.7; Cl, 12.3; Mn, 19.1; Found (%) C, 29.0; H, 3.4; N, 4.5; S, 2.4; Cl, 12.1; Mn, 18.8, IR (KBr pellet cm^{-1}): 1435 *ν* (C–O); 1499 *ν* (N=N); 1590 *ν* (C=O); 570 *ν* (M–O); 485 *ν* (M–N).

$[Zn_4(BDHAPADPS)Cl_4(H_2O)_4]$ (Brown) $C_{28}H_{26}Cl_4Zn_4N_4O_{12}S$ (1045.8), m.p. > 250 °C, Anal Calc. (%) C, 32.1; H, 2.5; N, 5.3; S, 3.0; Cl, 13.5; Zn, 25.0; Found (%) C, 31.8; H, 2.2; N, 5.1; S, 2.8; Cl, 13.2; Zn, 24.8, IR (KBr pellet cm^{-1}): 1436 *ν* (C–O); 1498 *ν* (N=N); 1592 *ν* (C=O); 530 *ν* (M–O); 482 *ν* (M–N).

$[Cd_2(BDHAPADPS)Cl_4(H_2O)_4]$ (Grey) $C_{28}H_{26}Cl_4Cd_4N_4O_{12}S$ (1234.0), m.p. > 250 °C, Anal Calc. (%) C, 27.2; H, 2.1; N, 4.5; S, 2.5; Cl, 11.4; Cd, 36.4; Found (%) C, 27.1; H, 2.0; N, 4.2; S, 2.3; Cl, 11.2; Cd, 36.1, IR (KBr pellet cm^{-1}): 1435 *ν* (C–O); 1500 *ν* (N=N); 1590 *ν* (C=O); 525 *ν* (M–O); 485 *ν* (M–N).

2.4 Physical Measurements

The metal contents of the complexes were determined by EDTA complexometric titration method. Micro analysis of C, H and N was performed on a Perkin–Elmer 2400 analyser. The magnetic susceptibility was measured at RT by Gouy method. Conductance of the complexes were measured by using Toshniwal CL 01–06 Conductivity Bridge. FTIR spectra were recorded using 200i FT-IR Microscopy System. Electronic spectra of Co^{II}, Ni^{II} and Cu^{II} complexes in DMF were recorded on a Hilger-Watt uvispeck spectrophotometer. ESR spectrum of Cu^{II} complex was recorded on an E_4—spectromete. ^1H NMR and ^{13}C NMR spectra were recorded on a Jeol GSX 400 with $CDCl_3$ as solvent and TMS as internal standard. The Electron Spray Ionization–Mass Spectrometric (ESI–MS) analysis was carried out by micrOTOF-Q ‖ 10337. X-ray diffraction study of the Ni^{II} complex was recorded on a Phillips PW 1130/00 diffractometer with scan axis-Gonio, start position (2θ-10.004) end position (2θ-89.976) anode material CuK—ALPHA 1[Å] = 1.54060 and the generator settings 30 mA, 40 kV. The Scanning Electron Microscope (SEM) of make JEOL instrument model JSM-5410 was used to determine the microstructure of complexes. Energy Dispersive X-ray (EDX) analysis was done by EDX (TESCAN) X-max version 4.1.17.D/Mi 152. TG, DTG and DTA of the Co^{II} complex was recorded on NETZSCH STA 409 C/CD in a nitrogen atmosphere at a heating rate of 10 °C per minute.

2.5 Theoretical (DFT/B3LYP) Studies

The optimized geometry of the azo dye ligand and its Cu^{II} and Zn^{II} complexes were studied with Gauss View 5.0.8 [7]. The theoretical calculations were made using GAUSSIAN 03 rev. A.01 programme package [8–14] hybrid DFT/B3LYP hybrid functional level of theory with LANL2DZ basic set for copper and zinc atoms in gas phase and 6-31 G(d, p) basic set for other atoms.

2.6 Antibacterial Activity

The antibacterial activity of the azodye ligand and five complexes was studied as per the cup-plate method using seven strains of bacteria, two Gram positive and five Gram negative. The solutions were prepared in dimethylsulphoxide (DMSO) at 500 µg/mL. The bacterial strains were inoculated into 100 mL of the sterile nutrient broth and incubated at 37 ± 1 °C for 24 h. The density of the bacterial suspension was standardised by McFarland method. A well of uniform diameter (6 mm) was made on agar plates, after inoculating them separately with the test organisms aseptically. The standard drug and the test compounds were introduced with the help of micropipette and the petriplates were placed in the refrigerator at 8–10 °C for proper diffusion of drug into the media. After 2 h of cold incubation, the petriplates are transferred to incubator and maintained at 37 ± 2 °C for 18–24 h. Then the petriplates are observed for zone of inhibition by using vernier scale. The results are reported by comparing the zone of inhibition shown by the test compounds with standard drug Tetracycline. The results are the mean value of zone of inhibition measured in millimetre.

3 Results and Discussion

Metal complexes were prepared according to the following reaction scheme:

$$4MCl_2 \cdot nH_2O + LH_4 \xrightarrow[\text{Ethanol, } 4NH_4OH]{\text{Heat, } 60-70\,^\circ C} [M_4LCl_4(H_2O)_{12}] + 4NH_4Cl$$

where, M = Co(II), Ni(II), Cu(II), Mn(II), LH_4 = BDHAPADPS.

$$4M'Cl_2 \cdot nH_2O + LH_4 \xrightarrow[\text{Ethanol, } 4NH_4OH]{\text{Heat, } 60-70\,^\circ C} [M'_4LCl_4(H_2O)_4] + 4NH_4Cl$$

where, M = Zn(II), Cd(II), LH_4 = BDHAPADPS.

Elemental analysis data agree well with the following composition of the metal complexes $[M_4LCl_4(H_2O)_{12}]$ and $[M'_4LCl_4(H_2O)_4]$ where M = Co^{II}, Ni^{II}, Cu^{II} Mn^{II}; M′ = Zn^{II}, Cd^{II}. All the complexes are amorphous in nature and have high melting points. The complexes are insoluble in common organic solvents but soluble in dimethylformamide and dimethyl sulfoxide. The complexes are non-electrolytic in nature as evident from their low conductance values (3.5–5.4 Ω^{-1} cm^2 mol^{-1}) in 10^{-3}M DMF solution.

3.1 IR Spectra

The sharp bands observed at 1607 cm^{-1} and 1631 cm^{-1} in the ligand can be ascribed to $\nu_{(-N=N-)}$ and $\nu_{(C=O)}$ vibrations respectively. In the metal complex these bands are observed at ~ 1499 and ~ 1593 cm^{-1}, respectively indicating coordination of one of the azo nitrogens and carbonyl oxygen atoms to the metal ions [15]. The band appeared at 1475 cm^{-1} in the ligand, assigned to $\nu_{(C\text{-}O)}$ vibrations has been shifted to ~ 1435 cm^{-1} in the metal complexes which indicates the bonding of phenolic oxygen atom to the metal ions. In the metal complexes a broad band appeared at ~ 3389 cm^{-1} followed by sharp peaks at ~ 840 and ~ 683 cm^{-1} assignable to –OH stretching, rocking and wagging vibrations, respectively indicating the presence of co-ordinated water molecules [16]. The conclusive evidence of bonding of the ligand to the metal ions is proved by the appearance of bands at ~ 576 cm^{-1} (M–O) and ~ 492 cm^{-1} (M–N) [17].

Table 1 Electronic spectra and magnetic moment data

Complex	ν in (cm^{-1})	Transition	μ_{eff} in BM	Dq in (cm^{-1})	B in (cm^{-1})	β_{35} in (cm^{-1})	ν_2/ν_1	σ in %
$[Co_4LCl_4(H_2O)_{12}]$	8250	$^4T_{1g}(F) \rightarrow {}^4T_{2g}(F)$ (ν_1)	5.0	828.5	816	0.840	2.004	19.04
	16,535	$^4T_{1g}(F) \rightarrow A_{2g}$ (F) (ν_2)						
	20,455	$^4T_{1g}(F) \rightarrow {}^4T_{1g}$ (P) (ν_3)						
	32,410	CT band						
$[Ni_4LCl_4(H_2O)_{12}]$	10,220	$^3A_{2g}$ (F) $\rightarrow {}^3T_{2g}$ (F) (ν_1)	3.1	1022	779.3	0.748	1.708	33.68
	17,460	$^3A_{2g}$ (F) $\rightarrow {}^3T_{1g}$ (F) (ν_2)						
	24,890	$^3A_{2g}$ (F) $\rightarrow {}^3T_{1g}$ (P) (ν_3)						
	32,860	CT band						
$[Cu_4LCl_4(H_2O)_{12}]$	13,375–14,480	$^2Eg \rightarrow {}^2T_{2g}$	1.78	–	–	–	–	–
$[Mn_4LCl_4(H_2O)_{12}]$	18,920	$^6A_{1g} \rightarrow {}^4T_{1g}$ (4G)	5.91	–	–	–	–	–
	21,150	$^6A_{1g} \rightarrow {}^4E_g, {}^4A_{1g}$ $^4A_{1g}$ (4G) (10B + 5C)						
	31,750	$^6A_{1g} \rightarrow {}^4E_g$ (4D) (17B + 5C)						
	37,440	$^6A_{1g} \rightarrow {}^4T_{1g}$ (4P)						

3.2 Electronic Spectra and Magnetic Measurements

In the electronic spectrum of Co^{II} complex, four ligand field bands appeared at 8250, 16,535, 20,455 and 32,410 cm^{-1}, assignable to $^4T_{1g}(F) \rightarrow {}^4T_{2g}(F)$ (ν_1), $\rightarrow {}^4A_{2g}(F)$ (ν_2) and $\rightarrow {}^4T_{1g}(P)$ (ν_3) and CT transitions [18, 19], respectively. The ligand field parameters as Dq = 828.5 cm^{-1}, B = 816 cm^{-1}, $\beta_{35} = 0.840$ cm^{-1}, $\nu_2/\nu_1 = 2.004$ and $\sigma = 19.04\%$ have been calculated which suggest an octahedral geometry for the complex [20, 21]. In the electronic spectrum of Ni^{II} complex, four ligand field bands were observed at 10220, 17460, 24890 and 32860 cm^{-1} assignable to $^3A_{2g}(F) \rightarrow {}^3T_{2g}(F)$ (ν_1), $\rightarrow {}^3T_{1g}(F)$ (ν_2), $\rightarrow {}^3T_{1g}(P)$ (ν_3) and CT transition, respectively [18], The ligand field parameters as Dq = 1022 cm^{-1}, B = 779.3 cm^{-1}, $\beta_{35} = 0.748$ cm^{-1}, $\nu_2/\nu_1 = 1.708$ and $\sigma = 33.68\%$ have been calculated. Which

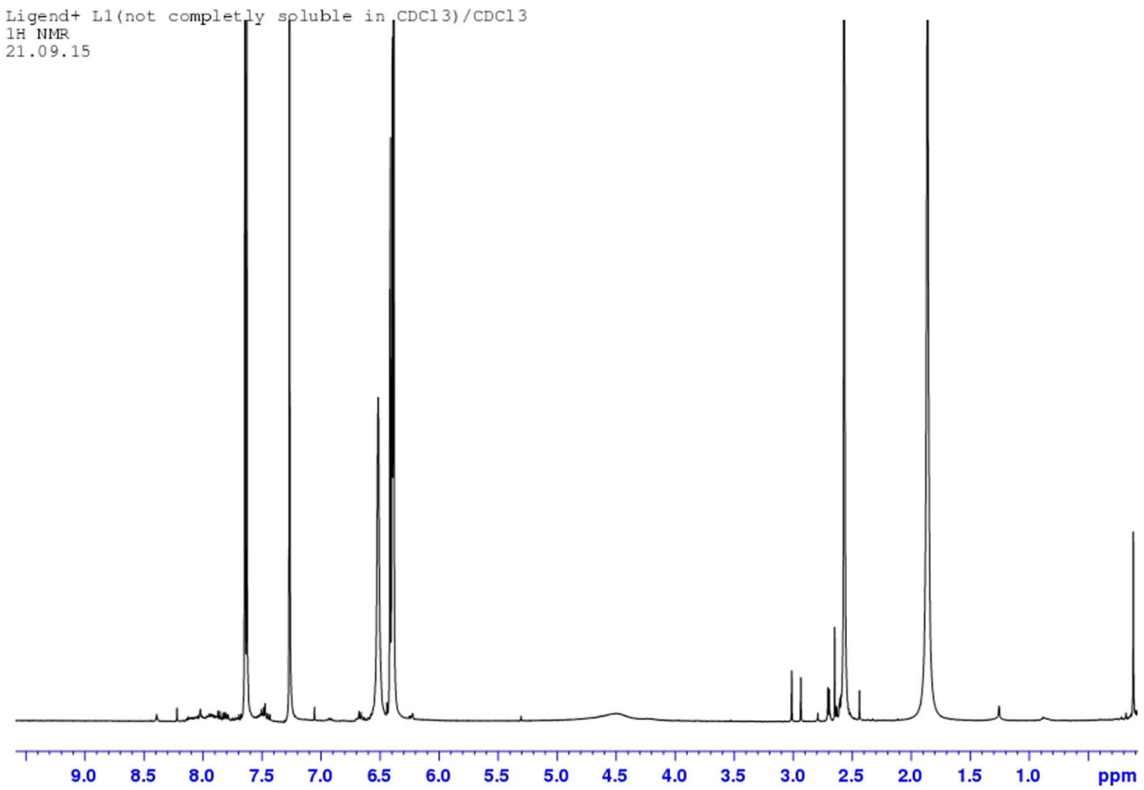

Graph 1 ^1H NMR spectrum of LH_4

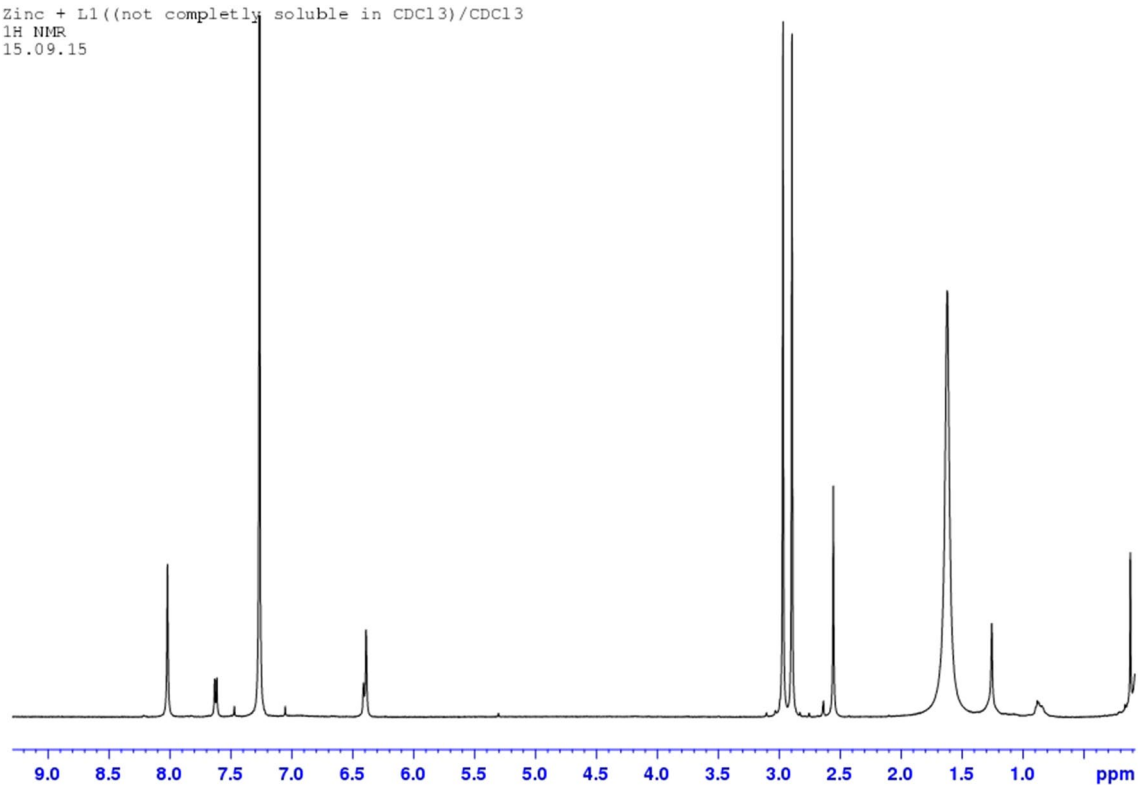

Graph 2 ^{1}H NMR spectrum of Zn (II) complex

suggest an octahedral configuration for the complex. The electronic spectrum of the Cu(II) complex shows one broad band at ~ 13,375–14,480 cm^{-1} with maxima at ~ 14,360 cm^{-1} assignable to $^{2}Eg \rightarrow {}^{2}T_{2g}$ transition in support of a distorted-octahedral geometry for the complex [22, 23]. The electronic spectrum of the Mn(II) complex shows four weak intensity bands at 18,920, 21,150, 31,750 and 37,440 cm^{-1} characteristics of octahedral geometry [24] which may be assigned to $^{6}A_{1g} \rightarrow {}^{4}T_{1g}$ (^{4}G), $\rightarrow {}^{4}E_{g}$, $^{4}A_{1g}$ (^{4}G), $\rightarrow {}^{4}E_{g}$ (^{4}D) and $^{4}T_{1g}$ (^{4}P), respectively.

The magnetic moment values of Co^{II}, Ni^{II}, Cu^{II} and Mn^{II} complexes are found to be 5.0, 3.1, 1.78 and 5.91 B.M., respectively indicating octahedral environment around the metal ions [25, 26] (Table 1). These four complexes are no doubt tetranuclear in nature, they exhibit normal magnetic moments due to absence of M–M interaction among the metal ions.

3.3 ^{1}H-NMR Studies

A complex pattern observed at δ 6.41–7.61 ppm corresponds to twelve phenyl protons [27]. The sharp peak at δ 2.63 ppm corresponds to six methyl protons (Graph 1). The signal observed at 3.0 ppm with an integration corresponding to eight protons in case of Zn(II) complex is assigned to four water molecules [28] (Graph 2).

3.4 ^{13}C NMR Analysis

As given in the (Graph 3) the ^{13}C NMR signal for the carbon of methyl group (C-1) of the ligand appeared at 26.0 ppm (Table 2). The signal for the carbon atom of the carbonyl group (C-2) appeared at 203.0 ppm. The carbon signals of C–O groups are shown at 163.0 and 166.0 ppm. Aromatic carbons signals appeared in the range 103–133.0 ppm. In the Zn(II) complex the signal due to carbonyl carbon and the carbon bonded to phenolic –OH groups are slightly shifted downfield thereby conforming the formation of coordination bonds between zinc and carbonyl oxygen and phenolic oxygen atoms [29] (Graph 4). Thus ^{1}H and ^{13}C NMR results confirm the proposed structure of the azodye ligand ad its complexes.

3.5 ESR Studies

The E.S.R. spectrum of copper(II) complex has been recorded at X-band at RT. The g_1, g_2 and g_3 values are found at 2.0269, 2.0898 and 2.2548, respectively [30]. The axial

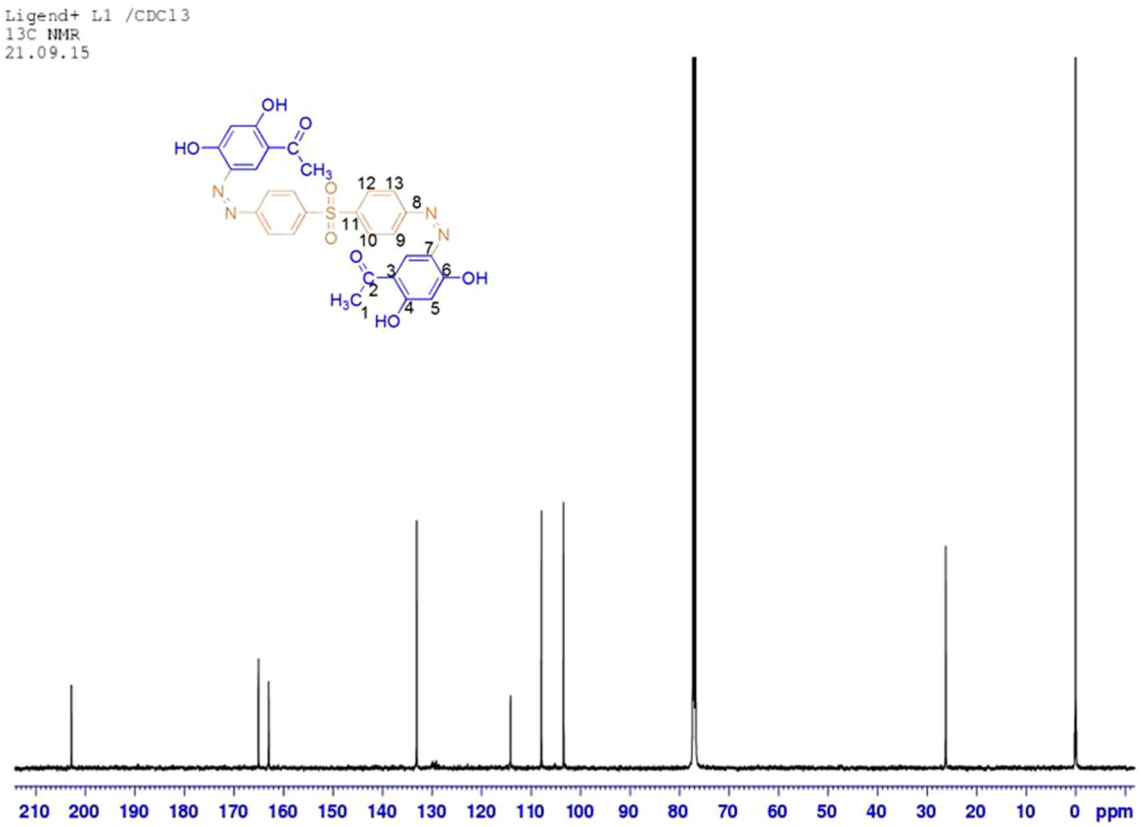

Graph 3 ^{13}C NMR spectrum of LH_4

Table 2 Selected bond length (Å) and bond angle (°) of the ligand (LH_4)

Bond length (Å)	Bond angle (°)
B3LYP/6.31G (d, p)	
N52–N53 (1.216)	N52–N53–C24 (120.002)
C24–N53 (1.301)	C24–C26–O59 (120.018)
C24–C26 (1.385)	C2–N8–N13 (120.018)
C26–O59 (1.410)	C23–C28–O58 (119.999)
C28–O58 (1.410)	C27–C10–O57 (120.024)
C10–O57 (1.212)	
C10–C27 (1.539)	

symmetry parameter "G" for the complex is found to be 4.363 which indicates that the absence of exchange interaction among magnetically equivalent Cu(II) ions in the unit cell. In order to obtain information about the ground state another useful parameter "R" can be calculated by using equation.

$$R = \frac{g_2 - g_1}{g_3 - g_2}$$

The "R" value is found to be less than one (0.3812), Hence the ground state is predominantly d^{22}_{x-y}. The ϰ value of the complex is found to be − 372.18 cm^{-1}. The spin–orbit coupling constant (ϰ) can be calculated from the relation [31].

$$g_{av} = 2(1 - 2\lambda/10Dq)$$

The decrease of the ϰ value (− 3811 cm^{-1}) from the free ion value (− 830 cm^{-1}) indicates the overlapping of metal ligand orbitals in the metal complex (Graph 5).

3.6 Mass Spectra

In the ESI–MS spectrum of the ligand LH_4 displayed, a peak with *m*/*z* 577.4 corresponding to the molecular mass of the ligand (Graph 6). A peak with *m*/*z* 543.3 was also observed which may be formed due to the loss of two methyl groups. The sharp peak obtained with *m*/*z* 511.2 corresponds to the loss of two carbonyl oxygen atoms. The peak with *m*/*z* 487.3 is due to loss of both the carbonyl carbon atoms. Other fragmentation peaks pattern cannot be reported because it is beyond the range of the instrument used.

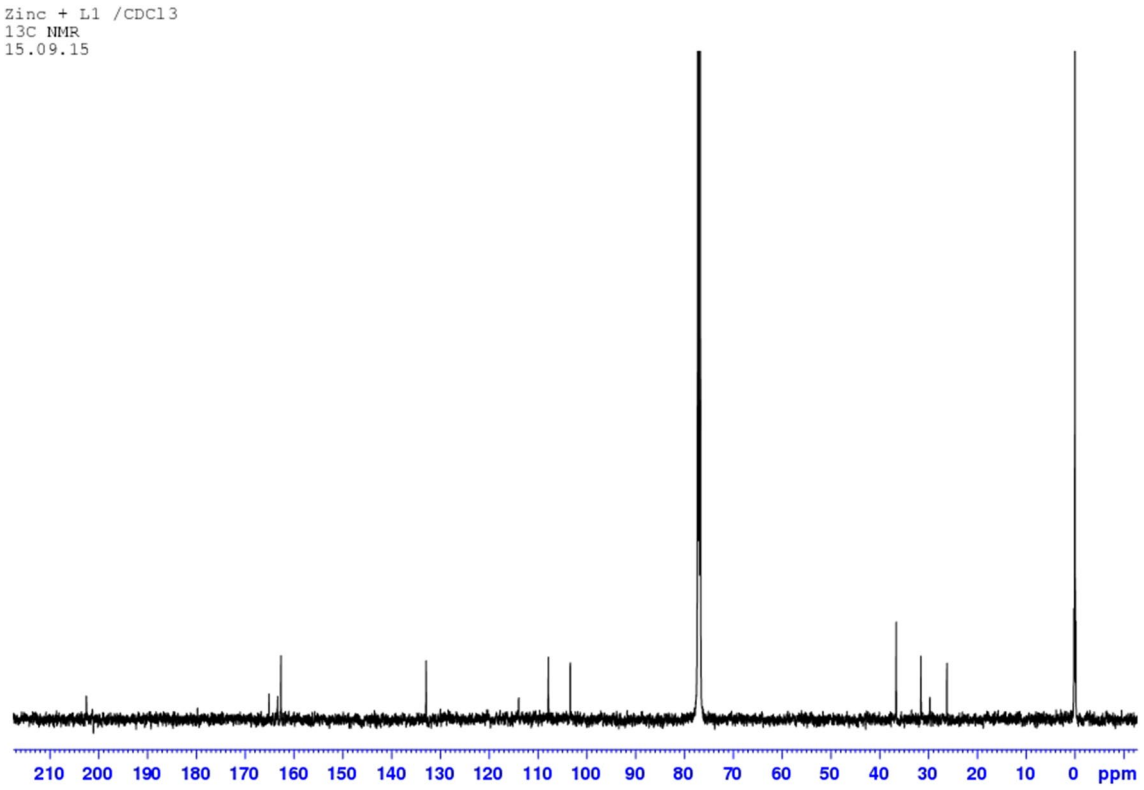

Graph 4 ^{13}C NMR spectrum of Zn (II) complex

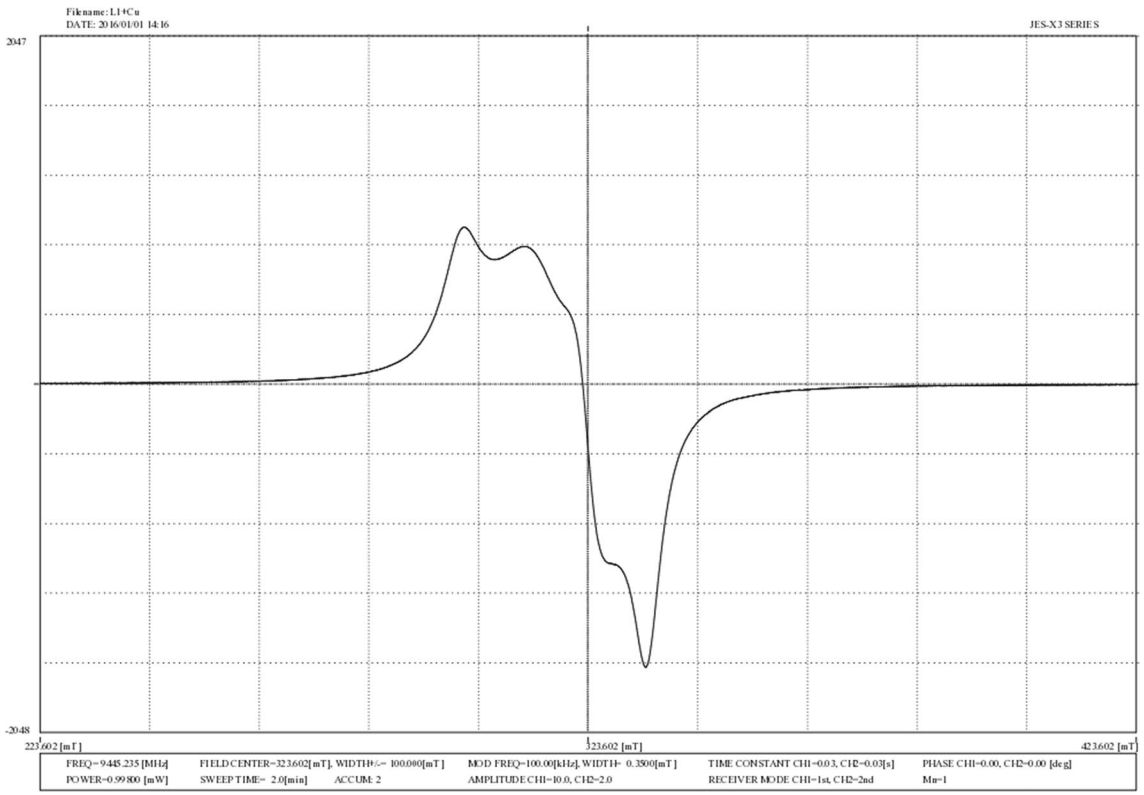

Graph 5 ESR spectrum of $[Cu_4LCl_4(H_2O)_{12}]$

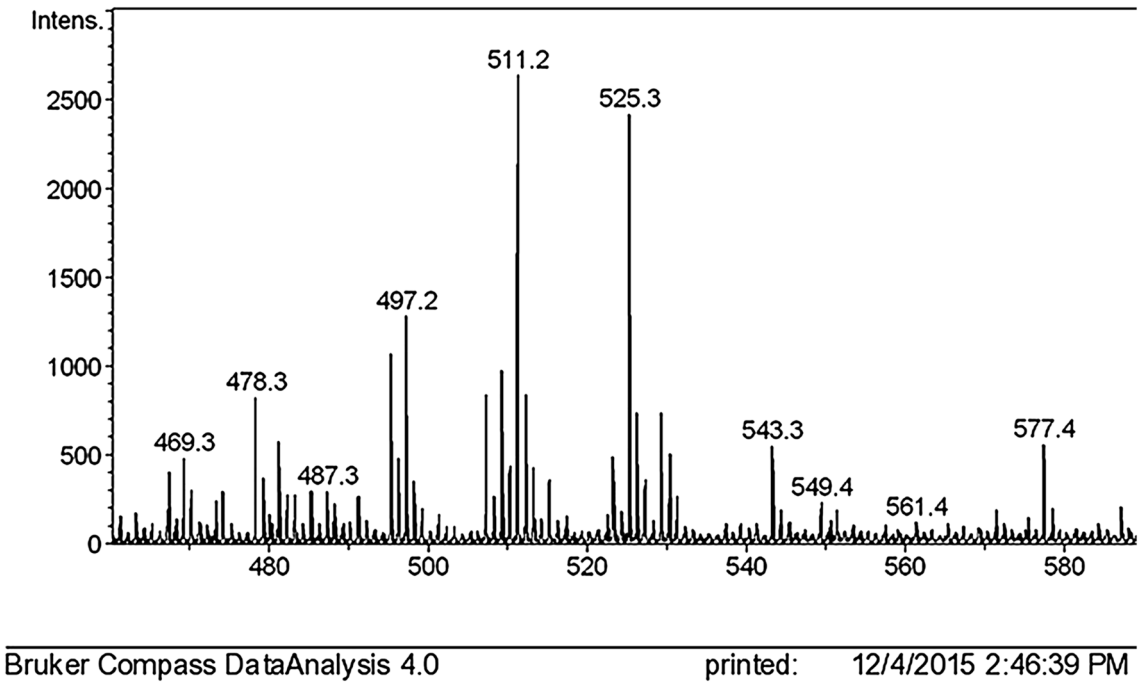

Graph 6 ESI–MS spectrum of LH_4

3.7 Powder XRD Studies

The XRD (powder pattern) of the complex $[Cd_4LCl_4(H_2O)_4]$ was indexed in X-ray diffractometer. The prominent peaks (Graph 7) of the diffraction pattern were indexed and analysed by the computer programme LSUCRPC [32]. The indexing is confirmed by comparing with observed and calculated 2θ values that are evident from the figure of merit 6.9 as suggested by de Woulff [33]. The observed and calculated 2θ values are also in good agreement. The density (d) of the complex was determined by floatation method in a saturated solution of KBr, NaCl and benzene separately. The number of formula units per unit cell (n) is calculated from the relation

$$n = \frac{dNV}{M}$$

where d = density of the complex, N = Avogadro's number, V = Volume of the unit cell and M = molecular weight of the complex. The value of 'n' is found to be 0.5 that agrees well with the suggested triclinic structure of the complex. The mean particle size of the same complex can be measured from the Debye–Scherrer equation

$$D = K\lambda/\beta \mathrm{Cos}\ \theta$$

where D = particle size, K = dimensionless shape factor, ƛ = X-ray wavelength, β = line broadening at half the maximum intensity, θ = diffraction angle. This equation relates the size of the particle in a solid in the broadening of a peak in a diffraction pattern. The particle size of the complex $[Cd_4LCl_4(H_2O)_4]$ is found to be 9.7 nm [34].

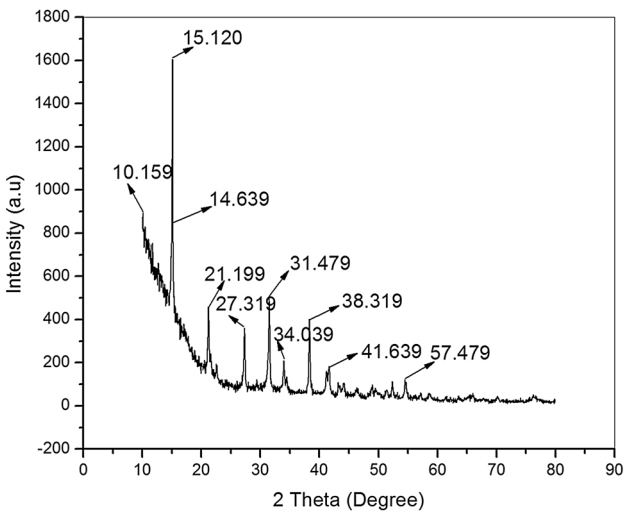

Graph 7 XRD graph of $[Cd_4LCl_4(H_2O)_4]$

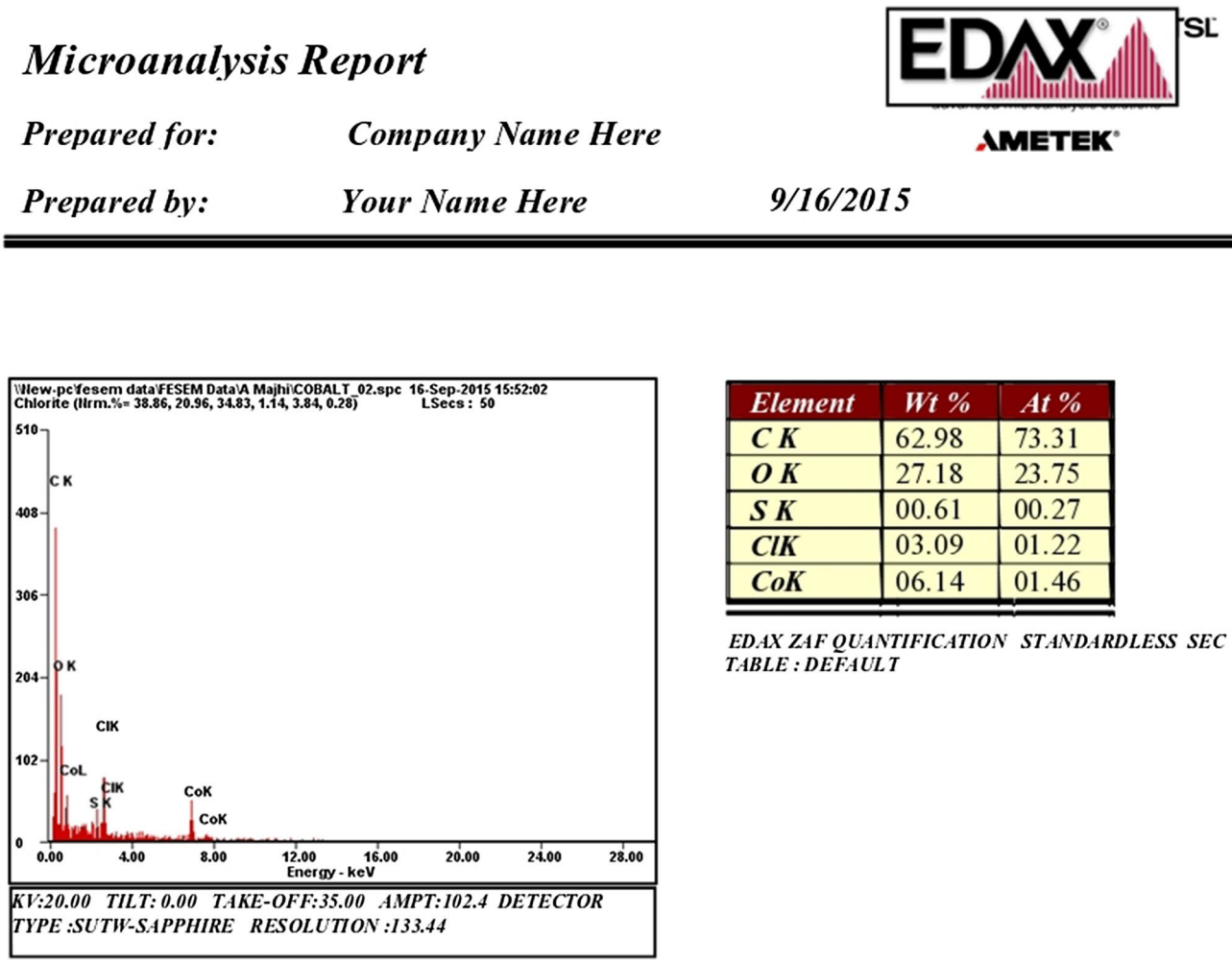

Fig. 2 EDX microanalysis spectrum of $[Co_4LCl_4(H_2O)_{12}]$

3.8 SEM and EDX Spectra

The two SEM micrographs of $[Co_4LCl_4(H_2O)_{12}]$ were recorded at 500 nm and 1 µm. It provides the surface morphology of the compounds. The SEM micrographs show rock shaped structure. The energy dispersive X-ray (EDX) analysis of the $[Co_4LCl_4\ (H_2O)_{12}]$ complex indicates the presence of Co, Cl, S, O and C as shown in (Fig. 2)

3.9 Thermogravimetric Studies

Thermal behaviour of $[Co_4LCl_4\ (H_2O)_{12}]$ was studied by TGA and DTA in the temperature range of ambient temperature to 900 °C (Graph 8). Initially the complex being stable up to 139 °C suffered a mass loss of 11.5% that corresponds to loss of six coordinated water molecules and it is supported by an endothermic peak at 138 °C. Thereafter, the compound looses a mass of 3.4% at 196 °C which corresponds to loss of another two coordinated water molecules from the complex which is supported by the endothermic peak on the DTA curve at 196 °C. Then, the compound gradually starts losing its weight with the rise of temperature and at 316 °C looses 17% of its weight which corresponds to the loss of rest of four coordinated water molecules and it is supported by the endothermic peak at 315 °C. Then the compound looses 11.4% at 461 °C which corresponds to the loss of two coordinated chlorine atoms and part of the ligand and it is supported at 460 °C on the DTA curve. Then the compound looses 10% of the weight at 535 °C which corresponds to loss of two coordinated oxygen atoms from ligand supported by the endothermic peak at 534 °C. Thereafter, the compound gradually losses almost all its masses and at 647 °C it form of CoO. Finally, the thermogram becomes a straight line after 647 °C.

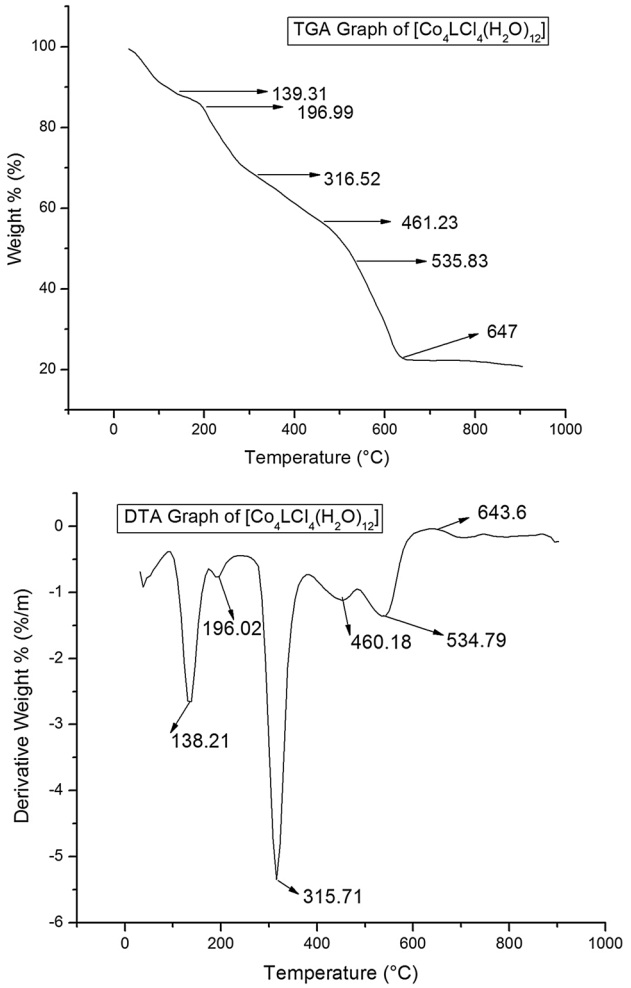

Graph 8 TGA and DTA graphs of $[Cd_4LCl_4\ (H_2O)_4]$

Kinetic parameters such as order of the reaction (n) and activation energy (E_a) can be calculated by Freeman-Carrol method [35]. Given below is the equation for this purpose:

$$-dw/dt = R_T = Z/R_H e^{-Ea/RT} W^n$$

where, R_H = rate of heating, W = weight fraction of the reacting material, E_a = activation energy and Z = frequency factor. This equation in the difference form can be written as

$$\Delta \log R_T = n\Delta \log W - E_a/2.303R\Delta(1/T)$$

When $\Delta\ (^1/_T)$ is kept constant, a plot of Δ log R_T verses Δ log W gives a linear relationship whose slope and intercept provide the value of n and E_a respectively. The order of decomposition reaction and the activation energy are found to be 0.5 and 8.13 J/mole, respectively. The calculated value of activation energy is found to be low that shows autocatalytic effect of the metal ion [36]. The Correlation factor (r) is found to be 0.98 and the thermal decomposition of the complex fits well with the experimental results.

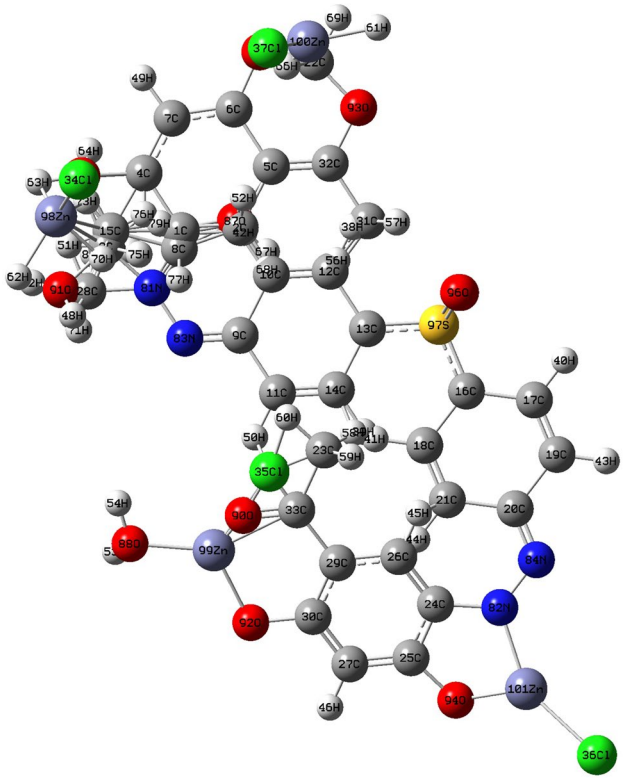

Fig. 3 Optimized geometry of the Zn (II) complex

Table 3 Selected bond length (Å) and bond angle (degree) of $[Zn_4LCl_4(H_2O)_4]$

Bond length (Å)	Bond angle (°)
$[Zn_4LCl_4(H_2O)_4]$ B3LYP/LANL2DZ	
N82–N84 (1.351)	Zn101–N82–C24 (110.995)
C24–N82 (1.446)	Zn101–O94–C2 (107.503)
C24–253 (1.386)	C2–C3–C25 (118.028)
C25–O94 (1.409)	N82–Zn101–Cl36 (148.670)
C30–O92 (1.409)	O94–Zn101–Cl36 (129.753)
C33–O90 (1.212)	Zn99–O92–C30 (109.511)
C29–C33 (1.539)	Zn99–O90–C33 (134.936)
Zn101–O94 (1.758)	O90–Zn99–Cl35 (170.979)
Zn101–N82 (1.925)	O92–Zn99–Cl35 (32.790)
Zn101–Cl36 (2.240)	
Zn99–O90 (1.063)	
Zn99–O92 (1.889)	
Zn99–Cl35 (2.239)	

3.10 Theoretical Calculation

3.10.1 Geometrical Optimization

The ligand LH_4 and $[Zn_4LCl_4(H_2O)_4]$ complex (Fig. 3) were optimized by using B3LYP/6-31G (d, p) and B3LYP/

Table 4 Energetic properties of the ligand (LH_4) and its $[Cu_4LCl_4(H_2O)_{12}]$ and $[Zn_4LCl_4(H_2O)_4]$ complexes calculated by DFT/B3LYP 6.31G (d, P) and DFT/B3LYP LANL2DZ basic sets

Compound	Single point energy in kcal/mol		Dipole moment (D)	
	DFT/B3LYP 6.31G (d, P)	DFT/B3LYP LANL2DZ	DFT/B3LYP 6.31G (d, P)	DFT/B3LYP LANL2DZ
LH_4	-8.9263×10^5	–	− 1.308	–
$[Cu_4LCl_4(H_2O)_{12}]$	-5.8367×10^6	-1.7568×10^6	− 0.514	− 0.663
$[Zn_4LCl_4(H_2O)_4]$	-7.2953×10^6	-1.6289×10^6	− 5.880	− 6.706

Table 5 Antibacterial activities of the ligand and the complexes (data presented as diameter of zone of inhibition in mm and % activity index)

Sl. no.	Compound	*Klebsiella*	*Salmonella*	*S. aureus* (MTCC-87)	*Bacillus*	*E. coli* (MTCC-40)	*P. Aeruginosa*	*Vibrio Cholerae*
1	LH_4	12	10	8	10	11	9	10
2	$[Co_4LCl_4(H_2O)_{12}]$	5	7	8	3	5	5	6
3	$[Ni_4LCl_4(H_2O)_{12}]$	10	8	5	6	–	6	7
4	$[Cu_4LCl_4(H_2O)_{12}]$	15	17	14	20	14	18	20
5	$[Mn_4LCl_4(H_2O)_{12}]$	20	16	15	12	15	10	14
6	$[Zn_4LCl_4(H_2O)_4]$	20	22	25	23	20	16	21
7	Tetracycline	30	30	30	30	30	30	30

LH_4 = 4,4′-bis(2,4′-dihydroxy-5′-acylphenylazo)diphenylsulphone (BDHAPADPS)

LANL2DZ basic sets to get the stable geometry. It is observed that the bond lengths and bond angles mentioned in Table 2 of the ligand have been changed in the metal complex (Table 3) indicating the bonding of ligand donor atoms with the metal ions [37, 38].

The single point energy and dipole moment value of LH_4, $[Cu_4LCl_4(H_2O)_{12}]$ and $[Zn_4LCl_4(H_2O)_4]$ are calculated using DFT/B3LYP 6-31G (d, p) and DFT/B3LYP LANL2DZ basic sets (Table 4). The single point energy of $[Zn_4LCl_4(H_2O)_4]$ is found to be less than the energy of the $[Cu_4LCl_4(H_2O)_{12}]$ which indicates the greater stability of the $[Zn_4LCl_4(H_2O)_4]$. In both basic set the higher dipole moment of $[Cu_4LCl_4(H_2O)_{12}]$ complex than the $[Zn_4LCl_4(H_2O)_4]$ complex indicates stronger dipole–dipole interaction in $[Cu_4LCl_4(H_2O)_{12}]$.

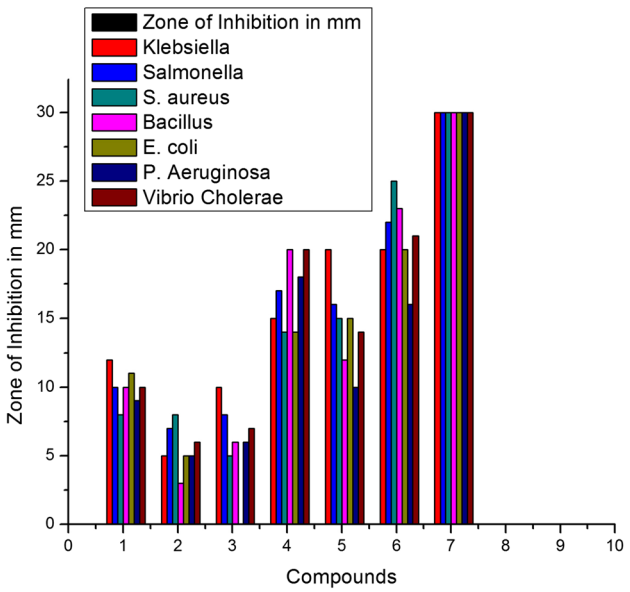

Graph 9 Effect of the complexes on the growth of selected bacteria

3.11 Antibacterial Activity

The ligand and metal complexes have been screened at 500 µg/ml for antibacterial activities and results are summarised in Table 5. The antibacterial activity of the compounds was examined against seven strains of bacteria, two gram positive *Staphylococcus aureus*, *Bacillus* and five Gram negative *Klebsiella, Salmonella, Pseudomonas Aeruginosa, Vibrio Cholerae* and *E. coli*. The drug Tetracycline is taken as standard to compare the effectiveness of the test compounds. It is observed that the zinc complex with the ligand is sensitive to almost all the bacteria. The zone of inhibition of tetracycline drug with the bacteria is found to be 30 mm each. The manganese and copper complexes are found to be intermediate against the bacteria. The other metal complexes are either less effective or resistant to the bacteria (Graph 9). The increased activity of metal chelate can be explained on the basis of the overtone concept and chelation theory [39]. The calculated partition coefficient (*C*

log *P*) of the Zn(II) complex (4.134) explains better biological activity as *C* log *P* is the major factor in the permeability of the tested compound through the cell membrane and can be directly related to the good biological effect. The Zn(II) complex is more potent than other complexes as indicated from its *C* log *P* value.

4 Conclusion

The octadentate ligand 4,4′-bis(2,4′-dihydroxy-5′-acylphenylazo)diphenylsulfone and its six tetrameric complexes were synthesized and their structures have been confirmed by elemental analysis, I.R., electronic, ^{1}H NMR, ^{13}C NMR, SEM, EDX, ESI–MS and ESR spectra. The stability of the complexes was confirmed from the thermal study. The kinetic parameters as activation energy (E_a) and order of reaction (n) are determined from the thermal decomposition data. The XRD study shows that the Cd(II) complex is triclinic in nature. The theoretical study using DFT/B3LYP supports experimental evidences of the bonding sites of the ligand, geometry and the stability of the complexes. The quantum chemical parameters reported here will be helpful to the future investigators working in the field of drug designing. The antibacterial study of ligand and its five metal complexes were studied against two Gram positive and five Gram negative bacteria.

Acknowledgements The authors are thankful to I.I.P Dehradun, India for providing spectral analysis, SEM, EDX, XRD and thermogravimetric analysis.

References

1. Dapsone (2015) The American Society of Health-System Pharmacists. Retrieved Jan 12
2. Zhu YI, Stiller MJ et al (2001) Dapsone and sulfones in dermatology: overview and update. J Am Acad Dermatol 45(3):420–434
3. Mahapatra BB, Mishra RR, Sarangi AK (2016) Bull Chem Soc Ethiop 30(1):87–100. https://doi.org/10.4314/bcse.v30i1.8
4. Mahapatra BB, Mishra RR, Sarangi AK (2016) J Saudi Chem Soc 20:635–643. https://doi.org/10.1016/j.jscs.2013.07.002
5. Mahapatra BB, Mishra RR, Sarangi AK (2013) J Chem. Article ID 653540. https://doi.org/10.1155/2013/653540
6. Mahapatra BB, Chaulia SN, Sarangi AK, Dehury SN, Panda JR (2015) J Mol Struct. https://doi.org/10.1016/j.molstruc.2015.01.030
7. GaussView 5.0 (2009) Gaussian Inc., Wallingford, CT, USA
8. Becke AD (1993) J Chem Phys 98(7):5648–5652
9. Lee CT, Yang WT, Parr RG (1988) Phys Rev B 37:785–789
10. Becke AD (1988) Phys Rev A 88:1053–1062
11. Hay PJ, Wadt WR (1984) J Chem Phys 82(1):270–276
12. Hay PJ, Wadt WR (1985) J Chem Phys 82:284–298
13. Hay PJ, Wadt WR (1985) J Chem Phys 82:299–310
14. Frish MJ et al (2004) GAUSIAN 03, Revision E.01. Gaussian Inc., Pittsburgh, PA
15. Mishra LK, Keshari BN (1981) Indian J Chem Sect A 28:883–887
16. King RB, Bisnette MB (1966) Inorg Chem 5:300–306
17. Nakamoto K (1978) Infrared and Raman spectra of inorganic and coordination compounds. John Wiley, NY, p 239
18. Ferraro JR (1971) Low frequency vibration of inorganic and coordination compound. Plenum press, New York, p 321
19. Atkins PJ, Shriver DF (1999) Inorganic chemistry, 3rd edn. W.H. Freeman and CO, New York
20. Lever ABP (1984) Inorganic electronic spectroscopy. Elsevier, Amsterdam, p 554
21. Magee R, Gordan L (1963) Talanta 10:967–971
22. Yamada S (1966) Coordination Chem Rev 1:415–418
23. Procter IM, Hathaway BJ, Nicholls P (1968) J Chem Soc A 1678–1683
24. Tavman A, Gürbüz D, Çinarli A, Tan SB (2015) Bull Chem Soc Ethiop 29(1):63–74
25. Williams DH, Fleming I (1994) Spectroscopic methods in organic chemistry, 4th edn. Tata Mc Graw Hill, p 1
26. Jacob W, Mukherjee R (2006) Inorg Chim Acta 359:4565–4573
27. Dash UN (1995) Analytical chemistry: theory and practice, 1st edn. Sultan Chand & Sons, pp 143–173
28. Salman RD, Farrant RD, Lindon JC (1991) Spectrosc Lett 24(9):1071–1078
29. Alaghar AMA (2014) Mol Struct 1072:103–113
30. Hathway BJ, Billing DE (1970) Coord Chem Rev 5:143–149
31. Dutta RL, Syamal A (1982) Elements of magnetochemistry. S. Chand & Company Ltd., p 96
32. Visser JW (1969) J Appl Crystal 2:89–95
33. de Woulff PM (1968) J. Appl. Crystal 1:108–113
34. Patterson A (1939) Phys Rev 56(10):978–985
35. Freeman ES, Carroll B (1958) J Phys Chem 62(4):394–397
36. Iimura A, Inoue Y, Yasumori I (1983) Bull Chem Soc Jpn 56:2203–2209
37. Yousef TA, Rakha TH, El Ayaan U, Abu El Reash GM (2012) J Mol Struct 1007:146–157
38. Yousef TA, Abu El-Reash GM, Rakha TH, El-Ayaan U (2011) Spectrochim Acta 83(1):271–278
39. Mohanan K, Devi SN (2006) Russian J Coord Chem 32:600–609